OLD DOMINION UNIVERSITY RESEARCH FOUNDATION

DEPARTMENT OF PHYSICS
SCHOOL OF SCIENCES AND HEALTH PROFESSIONS
OLD DOMINION UNIVERSITY
NORFOLK, VIRGINIA

Technical Report PTR 84-1

THEORETICAL STUDIES OF SOLAR-PUMPED LASERS

By

Wynford L. Harries, Principal Investigator

and

Zeng-Shevan Fong

Progress Report
For the period July 16, 1983 - January 15, 1984

Prepared for the
National Aeronautics and Space Administration
Langley Research Center
Hampton, Virginia

Under
Research Grant NSG 1568
W. E. Meador, Technical Monitor
Space Systems Division

January 1984

DEPARTMENT OF PHYSICS
SCHOOL OF SCIENCES AND HEALTH PROFESSIONS
OLD DOMINION UNIVERSITY
NORFOLK, VIRGINIA

Technical Report PTR 84-1

THEORETICAL STUDIES OF SOLAR-PUMPED LASERS

By

Wynford L. Harries, Principal Investigator

and

Zeng-Shevan Fong

Progress Report
For the period July 16, 1983 - January 15, 1984

Prepared for the
National Aeronautics and Space Administration
Langley Research Center
Hampton, Virginia

Under
Research Grant NSG 1568
W. E. Meador, Technical Monitor
Space Systems Division

Submitted by the
Old Dominion University Research Foundation
P. O. Box 6369
Norfolk, Virginia 23508

January 1984

TABLE OF CONTENTS

TABLE OF CONTENTS - CONTINUED

LIST OF TABLES

LIST OF FIGURES

LIST OF FIGURES - CONCLUDED

SECTION III

SECTION IV

THEORETICAL STUDIES OF SOLAR PUMPED LASERS

By

Wynford L. Harries[1] and Zeng-Shevan Fong[2]

SUMMARY

The investigations of an IBr solar pumped laser have resulted in a publication "Kinetic Modeling of an IBr Solar pumped Laser" by W. L. Harries and W. E. Meador which will appear in the next issue of Space Solar Power Review. Work on the solar pumped laser has ceased and, for the period July 1983 to January 1984, attention was given to metal vapor lasers and, recently, black body pumped lasers. In addition, a calculation was made on a figure of merit, namely the power to weight ratio.

In the case of metal vapors, the possibility of using sodium and pumping a number of vibrational levels in the upper state which would relax to the upper level was treated in the last progress report.(1) It was shown that the efficiency would be small because of quenching. Another problem was self absorption at the laser frequency which would apply to any type of laser. The problem of self absorption and stimulated emission in sodium is treated in Section I of this report.

A second problem with metallic vapors especially in experimental work is the question of the ratio of dimers to monomers. A method of calculating

(1) "Theoretical Studies of Solar Pumped Lasers," W. L. Harries, PTR 83-4, July 1983.

[1] Eminent Professor, Physics Department, Old Dominion University, Norfolk, Virginia 23508.

[2] Graduate Research Assistant, Physics Department, Old Dominion University, Norfolk, Virginia 23508.

the ratio as a function of temperature is given in Section II.

A figure of merit for solar pumped lasers to be placed in orbiting space vehicles is the power to weight ratio, which should be as large as possible. A preliminary study was given in reference (1). This has been considerably extended, and now includes the effects of absorption by the container walls and collisions with dimers, for example. The new results are given in Section III.

Preliminary studies of black body pumped lasers have been started and a glossary of papers collected. It became apparent that there was a limitation to the scaling up of such lasers in cylindrical form and this is discussed in Section IV.

A preliminary study for carrying out some experimental measurements on metallic vapors has been undertaken.

I. STIMULATED EMISSION AND SELF ABSORPTION IN SODIUM VAPOR

1.1 Introduction

In any lasing medium the emission wavelength should be chosen where there is little self absorption. As emission and absorption spectra for metallic vapors did not seem available, therefore, estimates were made of these cross sections for sodium vapor as functions of wavelength. Although absolute values were not obtained, information on where the emission wavelength should occur became evident.

In section 1.2 the method of obtaining quantities proportional to the cross sections versus wavelength is outlined. A further comparison based on alternative expressions for the absorption and emission cross sections over a limited wavelength range is made in section 1.3 which supports the evidence of section 1.2.

1.2 Absorption and Emission Probabilities for Na_2 Vapor

The probabilities can be estimated if the Franck-Condon factors F(v", v') are known for transitions from the various vibrational levels v" in the ground state $X^1 \Sigma^+ g$ of Na_2, to vibrational levels v' in an electronically excited state. An excited state which would correspond to absorption in the visible is the $B'\Pi u$ and fortunately, a very complete table of Franck-Condon factors was given by Kusch and Hessel.[1] The amount of absorption from any level v" would depend on the relative population of the level to the other levels in the same electronic state. The levels would be filled according to Boltzmann statistics. Similarly the emission would depend on the relative population of the upper vibrational levels.

For the ground electronic state the energy of the level v" in cm^{-1}

was

$$E(v'') = W_e(v'' + \frac{1}{2}) - W_e x_e(v'' + \frac{1}{2})^2 \qquad (1)$$

where $W_e = 159.1\ cm^{-1}$, and $W_e x_e = 0.7254\ cm^{-1}$ and the lowest energy $E_0 = E(v'' = 0)$.[2]

The probability of filling level v'' was

$$P(v'') = \exp\left(\frac{E(v'')-E_0}{kT}\right) \qquad (2)$$

when k is Boltzmann's constant and T the temperature in degrees Kelvin. The fraction of molecules in this state was

$$f(v'') = P(v'') \Big/ \sum_{v''=0}^{n} P(v'') \qquad (3)$$

where n was taken as 45.

The minimum of the potential curve for the $B'\Pi u$ state was at 20,319 cm^{-1}, and the energy of the v' state was

$$E(v') = w_e'\,(v' + \frac{1}{2}) - w_e x_e'\,(v' + \frac{1}{2})^2 + 20{,}319 \qquad (4)$$

where $w_e' = 124.9\ cm^{-1}$, and $w_e x_e' = 0.6999$[2], and the lowest vibrational energy level $E_0' = E(v' = 0)$. The fraction of molecules filling level v',

namely $f(v')$ was calculated as in equations (2) and (3), except n was now taken as 28. The number n for both ground and excited electronic states was determined by the availability of Franck-Condon factors. Both numbers are sufficiently large so that inclusion of any higher levels would not change the results appreciably.

A quantity proportional to the absorption cross section, which is a function of wavelength λ is[3]

$$Q(\lambda) = F(v'', v')\, f(v'')\, \nu \qquad (5)$$

where ν is the frequency of the absorbing photon determined by $E(v') - E(v'')$. Plots of $Q(\lambda)$ is λ for transitions from level v'' to v' corresponding to $0 \leq v'' \leq 45$, $0 \leq v' \leq 28$ are shown in figure 1. The overall outline resembles a Gaussian absorption curve.

The values of $Q(\lambda)$ were then averaged over an interval of 5 nm to give smoother curves and are shown in figure 2 for temperatures of 500, 650 and 1000°C. The curves now resemble Gaussian absorption curves and increasing the temperature decreases the peak value and widens the wings, as it should.

An estimation of a quantity proportional to a stimulated emission cross section can be made in a similar manner. The probability of filling a vibrational level in the upper electronic state was again assumed to occur according to Boltzmann statistics. This assumption, however, may lead to error because the levels in the upper state are filled from the ground state, and their population densities are dependent on the rate of arrival from the ground state. If they remain in the upper state for many collisions, a Boltzmann distribution should result, but if they are quickly

quenched such a distribution is unlikely.

Assuming the fraction in level v', is $f(v')$ calculated as previously, then a quantity $R(\lambda)$ proportional to the stimulated emission cross section is given by[4]

$$R(\lambda) = F(v'', v')\, f(v')\, \nu^2 \qquad (6)$$

Plots of $Q(\lambda)$, $R(\lambda)$ vs λ are shown in figure 3. The values have been smoothed from those of figure 1 by averaging over a 5 nm bandwidth. It should be noted that for both quantities, the ordinate is arbitrary, and that they are only proportional to the absorption and stimulated emission cross sections. Hence, if figure 3 is regarded as a plot of the cross sections then they are not normalized with respect to each other. The temperature values are 600°C and 1000°C.

It is evident that the $R(\lambda)$ curve is shifted to the right of the $Q(\lambda)$ curve, suggesting a region between 500 and 540 nm where stimulated emission would dominate over self absorption.

1.3 Alternative Method of Comparing Emission and Absorption Cross Sections

The absorption cross section for a molecule is given by[5]

$$\sigma_a = \frac{A_{13}}{8\pi c^3}\, \lambda_a^2 \qquad (7)$$

where A_{13} is the Einstein coefficient for the transaction $1 \rightarrow 3$, λ_a is the absorption wavelength, and c the velocity of light. The emission cross section is given by

$$\sigma_e = \frac{\lambda_e^4 A_{32}}{4\pi^2 c \Delta\lambda_e} \qquad (8)$$

where λ_e is the emitted wavelength, A_{32} the Einstein coefficient for the transition from level 3, the upper lasing level to level 2 the lower lasing level $\Delta\lambda_e$ here is the emission bandwidth. If we consider the possibility of absorbing the wavelength λ_e, then $\lambda_a = \lambda_e$ and the ratio $\frac{\sigma_e}{\sigma_a}$ is then

$$\frac{\sigma_e}{\sigma_a} = \frac{2c^2}{\pi} \frac{A_{32}}{A_{13}} \frac{\lambda_e^2}{\Delta\lambda_e} \qquad (9)$$

and increases with λ_e^2. The expression may hold in the region between 5 and 5.4 nm in figure 3, but clearly does not hold elsewhere.

Assuming $\lambda_e = 525$ nm, $A_{13} = A_{32} = 1.9 \times 10^7$ s^{-1} and that $\Delta\lambda_e$ is determined by Doppler broadening, ($\Delta\nu = 3$ Ghz, $\Delta\lambda_e = 9.2 \times 10^{-13}$m)[5] then $\sigma_a = 6.9 \times 10^{-14}$ cm^2, $\sigma_e = 1.3 \times 10^{-12}$ cm^2 and the ratio $\frac{\sigma_e}{\sigma_e} = 19$.

1.4 Conclusions

The above independent check of the values of σ_e and σ_a in the wavelength range 5 to 5.4 nm showed $\frac{\sigma_e}{\sigma_a} = 19$. The plots of $Q(\lambda)$ and $R(\lambda)$ are not normalized, but at 5.25 nm show the ratio $\frac{R(\lambda)}{Q(\lambda)}$ to be about 3, suggesting the $R(\lambda)$ curve should be about six times higher. The form

of the curves show that the only region where lasing should be attempted in Na_2 is between 5.2 and 5.4 nm. This conclusion is consistent with the fact that lasing at 5.25 nm has been reported by Wellegehausen.[4]

REFERENCES - SECTION I

1. Kusch, P. and Hessel, M.M., J. Chem. Physics 68(6), 2591 (1978).

2. Huber, K.P. and Herzberg, G., "Molecular Spectra and Molecular Structure-Constants of Diatomic Molecules," Van Nostrand, 1978.

3. Herzberg, G., "Spectra of Diatomic Molecules," Van Nostrand, 2nd Edition, 1950, p. 383.

4. Ibid, p. 20.

5. Wellegehausen, B., I.E.E. J. Quantum Electronics QE-15, No. 8 (1979).

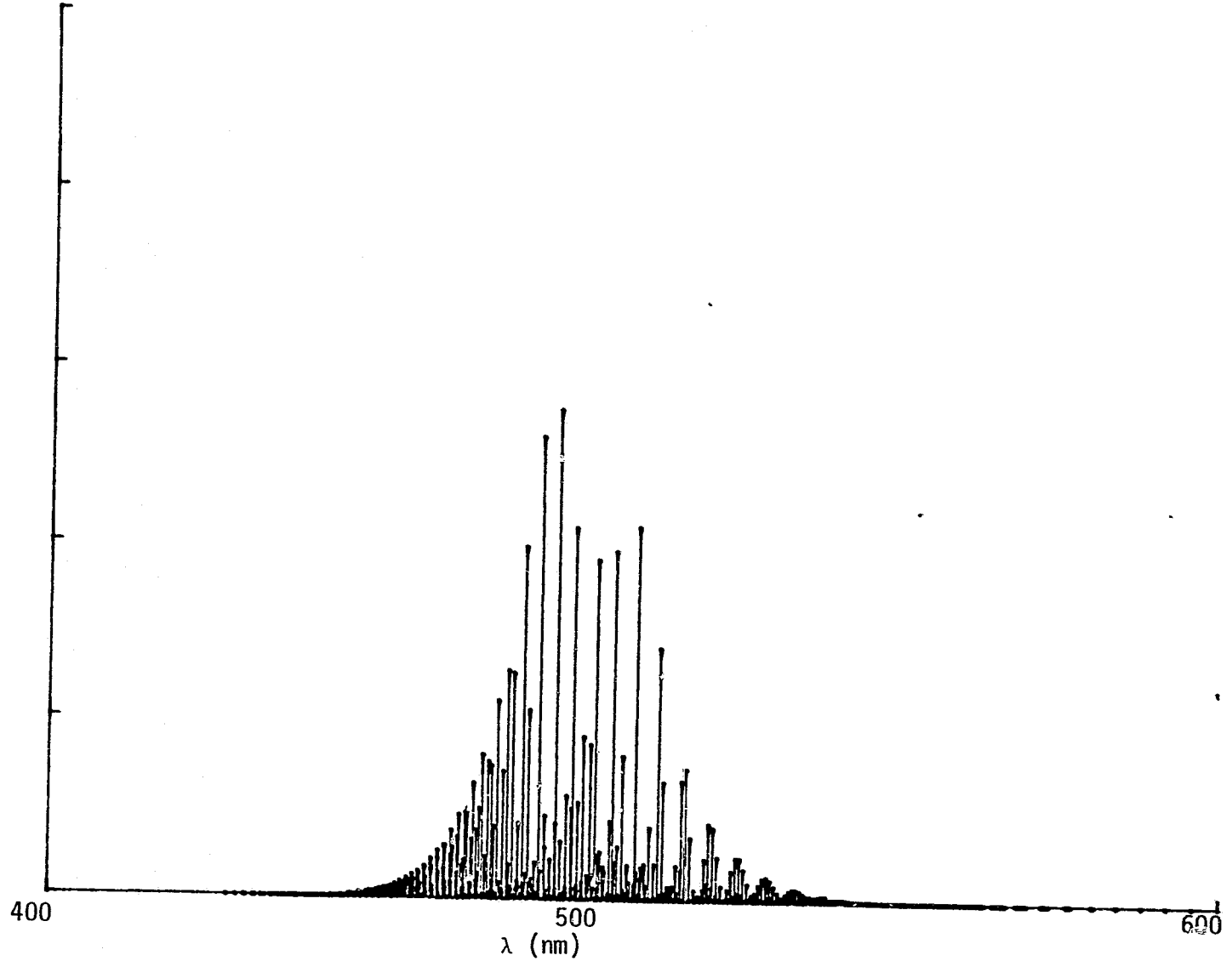

Fig. 1.1. Plot of $Q(\lambda)$ vs λ for Na_2 at 650^0C. The ordinate is arbitrary.

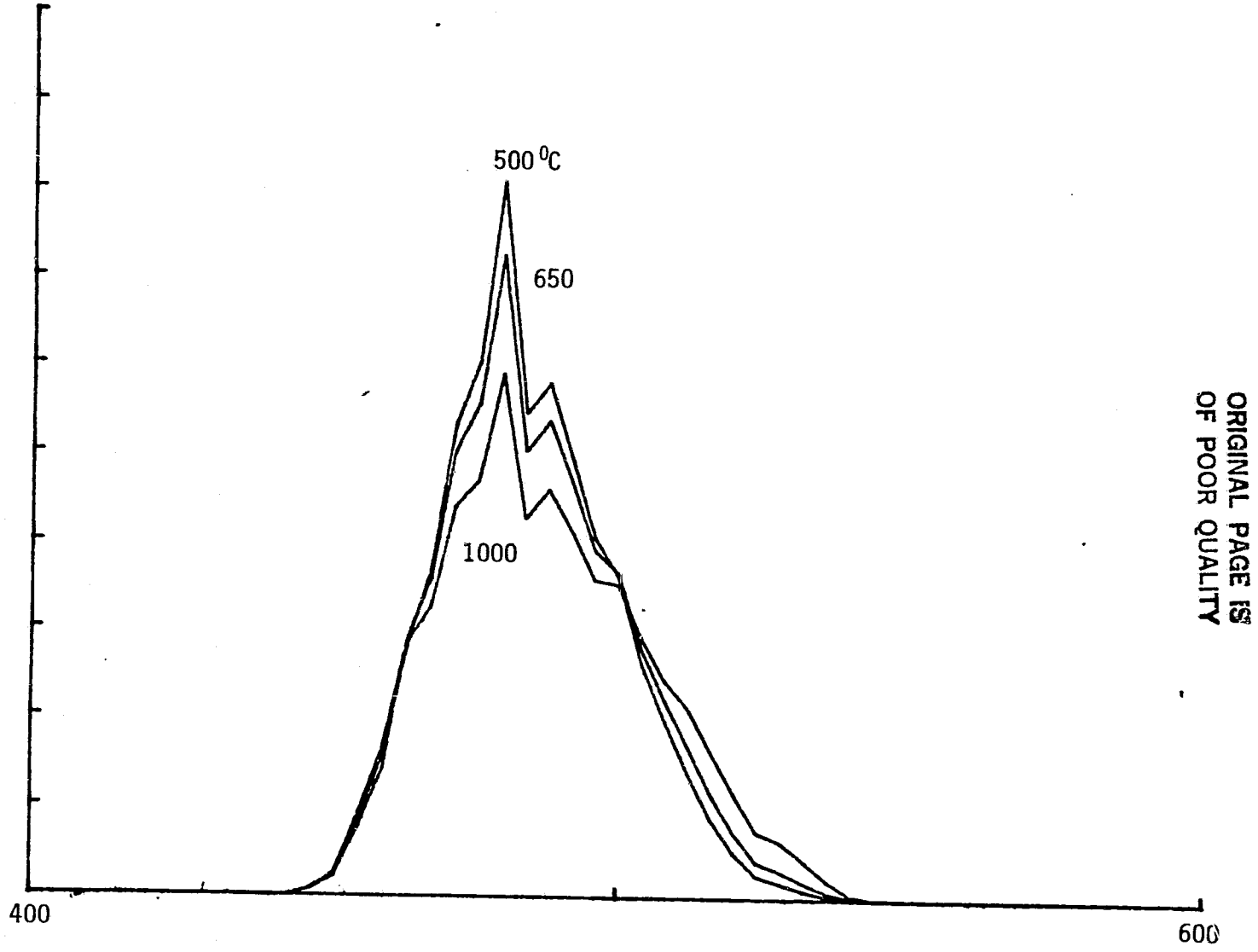

Fig. 1.2. Plots of $Q(\lambda)$ vs λ for different temperatures where the values have been averaged over 5 nm intervals.

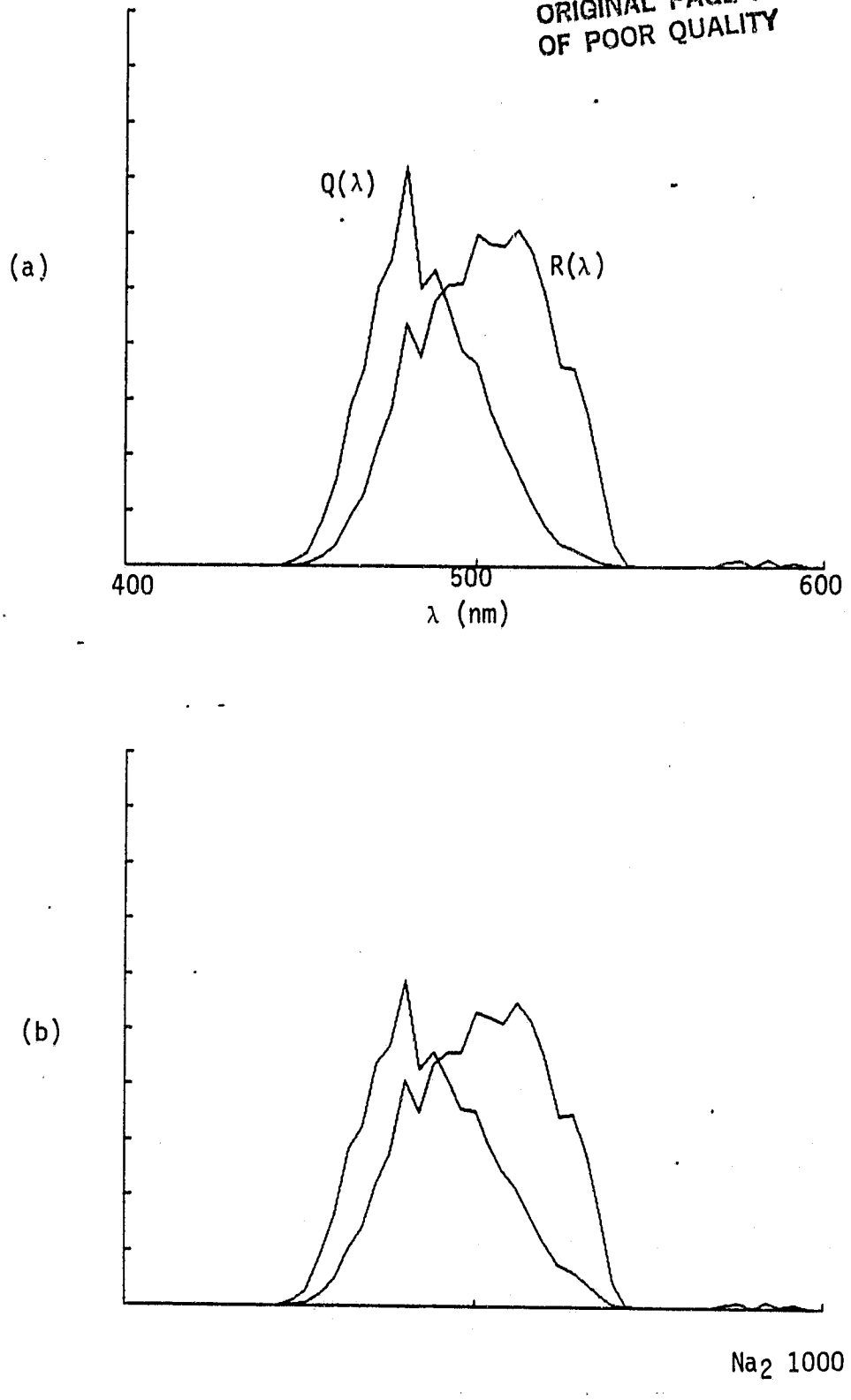

Fig. 1.3. Comparison of the quantities $Q(\lambda)$ and $R(\lambda)$ as functions of λ. The quantities are not normalized to each other, (a) T = 500°C, (b) T = 1000°C. The bandwidths are assumed to be 5 nm.

II. DENSITIES OF DIMERS AND MONOMERS IN METALLIC VAPORS

Summary

The dimer/monomer ratio is derived for metallic vapors as a function of temperature. The basic physical mechanisms are dissociation caused by collisions with energetic atoms, and three body recombination in the gas phase, and the creation of a saturated vapor at the gas-liquid interface. Increasing the temperature increases the collision and recombination rates so the dimer/monomer ratio rises. The effect of Na_2 acting as a third body in the recombination process is included for the first time.

2.1 Introduction

The possibility of using metallic vapors in lasers for solar energy conversion is appealing as they could operate at high temperatures. The lasing medium would be the dimers, which in many instances consist of only a small fraction of the gas particles. Plots of this fraction as a function of temperature were given by Lapp and Harris,[1] from results of Stull and Sinke[2] but without explanation. The purpose of this paper is to understand the processes which are occurring and to duplicate these results. The effect of the dimers acting as third bodies are included for the first time.

2.2 Physical Processes Occurring in Metallic Vapors

The vapor consists of a mixture of monomers and dimers boiled from the liquid phase, with a metallic wick connecting the regions of high and low temperatures. In the vapor phase it is assumed that the reactions of dissociation and recombination can occur as shown in table I.

Table I. Reactions Occurring in the Vapor Phase

Type of reaction		
Dissociation	a	$Na_2 + Na' \xrightarrow{k_f} Na + Na + Na$
Three body recombination	b	$Na + Na + Na \xrightarrow{k_r} Na_2 + Na$
	c	$Na + Na + Na_2 \xrightarrow{k_s} Na_2 + Na_2$

It is assumed that dissociation of Na_2 occurs according to reaction a in table I where k_f is the rate coefficient, and Na' is an atom with kinetic energy exceeding D_0, the dissociation energy of Na_2, and hence in the tail of a Maxwellian distribution:

$$Na'/Na = \exp(-D_0/kT) \tag{1}$$

Recombination in the gas occurs by three body collisions, and it will be assumed first that the predominating third body is Na, an assumption that works well at low temperatures as will be seen later. Hence, reaction b of table I dominates. The rate equation for Na_2 is then

$$\frac{d(Na_2)}{dt} = -k_f \, Na_2 \, Na' + k_r \, (Na)^3 \tag{2}$$

In the steady state, equations (1) and (2) yield

$$\frac{Na_2}{(Na)^2} = \frac{k_r}{k_f} \exp(D_0/kT) = K \tag{3}$$

where K is a constant for a given temperature.

Fortunately, reference (1) gave values of the partial pressures of dimers and monomers at a fixed temperature for several metals and if D_0 is known then the quantity k_r/k_f can be calculated. Equation (3) can then be used to calculate $Na_2/(Na)^2$ for any temperature.

The saturated vapor pressures of metals are well known and usually given in the form[3]

$$\log_{10} p = -\frac{0.05223}{T} a + b \qquad (4)$$

where p is in torr, T in degrees K and a and b are characteristic of the metal. The expression is valid from 180°C to 883°C.

The vapor pressure is also

$$p = (Na_2 + Na)\ kT \qquad (5)$$

and on rearranging equations (4) and (5)

$$Na_2 + Na = \frac{1}{kT} C \exp(-Q/kT) \qquad (6)$$

where C and Q are obtained from equation (4). Equations (3) and (6) then give solutions to Na, Na_2 and Na_2/Na.

Data for four metals are given in table II, and plots of Na_2/Na are shown in figure 1. The plots showed excellent agreement with the curves of

Stull and Sinke.[2] For all the vapors, the dimer-monomer ratio increases

Table II. Data for Metals

	Vapor pressure constants[3]		Partial Pressures at 700K (torr)[1,2]		D_0(eV)
	a	b	Monomer	Dimmer	
Na_2	103300	7.553	0.69	2.2×10^{-2}	0.730
Rb	76000	6.976	19.40	0.454	0.490
Cs	73400	6.949	27.60	0.625	0.450
K	84900	7.183	7.24	8.2×10^{-2}	0.510

with temperature. The reason is that at higher temperatures the densities of the particles increase and hence the recombination rate which is dependent on three body collisions increases faster than the dissociation rate.

Three body collisions where Na_2 is the third body have been neglected above. Also dissociative collisions from Na_2 molecules in the tail of the distribution. The error introduced is small within the temperature range of figure 1, as at most they constitute less than 8% of the total particles.

2.3 Effect of Na_2 as a Third Body

The Na_2 molecules acting as third bodies contribute an additional recombination reaction (c) to reaction (b) in table I. A rate coefficient k_s is introduced, different from k_r, but unfortunately the values of k_r, k_s are not known. The rate equation for Na_2 now becomes

$$\frac{d(Na_2)}{dt} = - k_f Na_2 Na' + k_r Na^3 + k_s Na^2 Na_2 \qquad (7)$$

and in the steady state, using equation (1), we obtain

$$\frac{Na_2}{Na^2 + \frac{k_s}{k_r} NaNa_2} = \frac{k_r}{k_f} \exp (D_o/KT) \qquad (8)$$

Equations (8) and (6) then given solutions of Na, Na_2 and Na_2/Na. Plots of Na_2/Na vs. temperature are shown in figure 2 for the case of sodium where the effect of the dimers as third bodies is shown in terms of a parameter α defined as $\alpha = k_s/k_r$. Thus when $\alpha = 0$ we revert to the case of Na_2 in figure 1. The temperature scale is shown to be 1000°C although the range of validity of equation (4) which leads to equation (6) is only up to 883°C. As the ratio k_r/k_s is not known, the behavior of k_s can only be illustrated by the parameters $\alpha = k_s/k_r$.

2.4 Conclusions

The dimer/monomer ratio calculated as a function of temperature for four different metal vapors showed excellent agreement with the curves of Stull and Sinke,[2] indicating that the dissociation three body recombination, and the creation of a saturated vapor were the basic processes occuring. Inclusion of the dimers as third bodies, in recombination collisions, increased the dimer/monomer ratio slightly, at higher temperatures.

REFERENCES - SECTION II

1. Lapp, M. and Harris, L.P., J. Quant. Spectroscopy Radiat. Transfer 6 169 (1966).

2. Stull, D.R. and Sinke, G.C., "Thermodynamic Properties of the Element," Adv. Chem Series. No. 18 (1956).

3. Handbook of Chemistry, 9th ed. edited by N. A. Lange, p. 1424 etc., Handbook Publishers Inc., 1956.

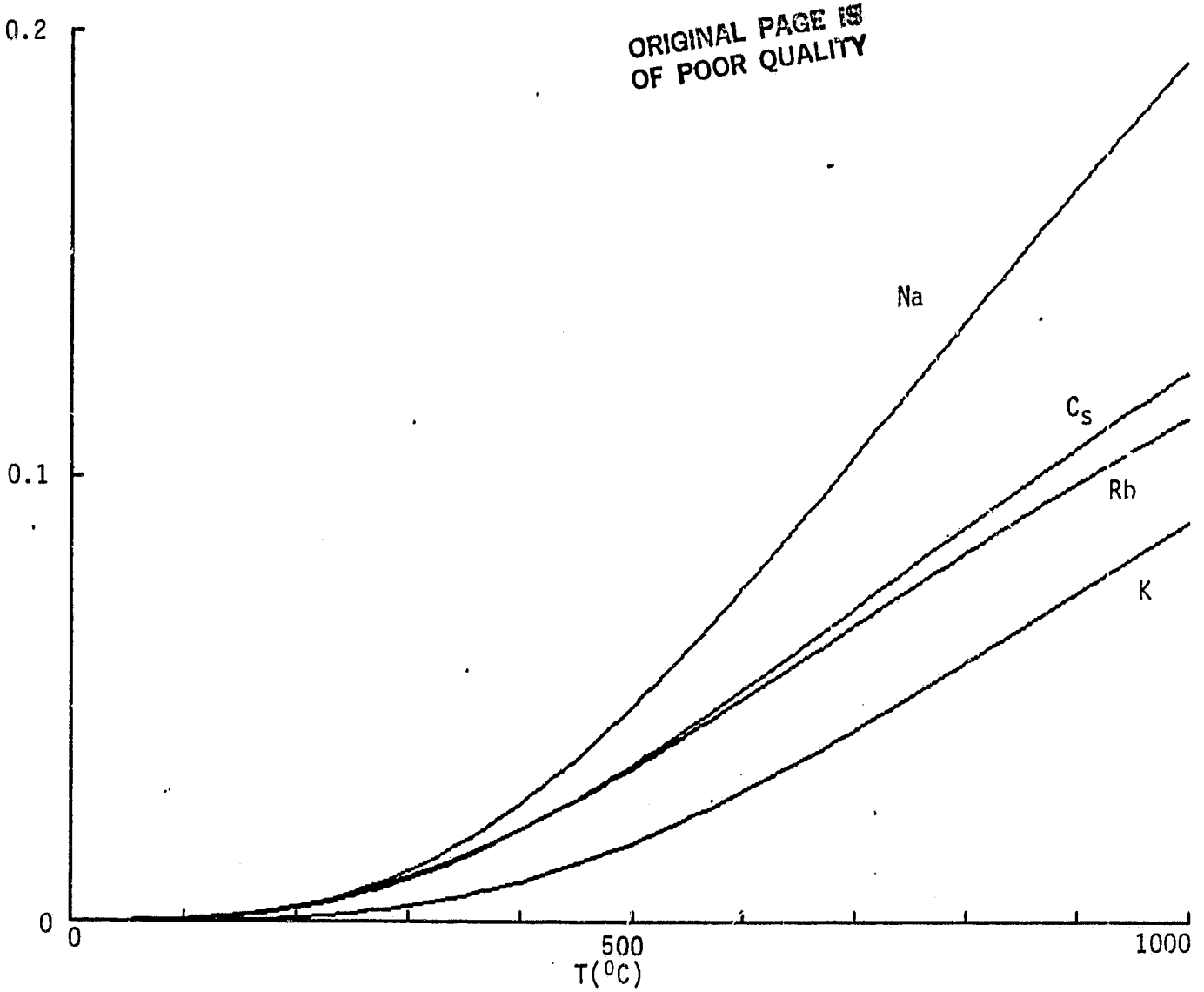

Fig. 2.1. Plots of dimer/monomer ratio vs T for different metal vapors.

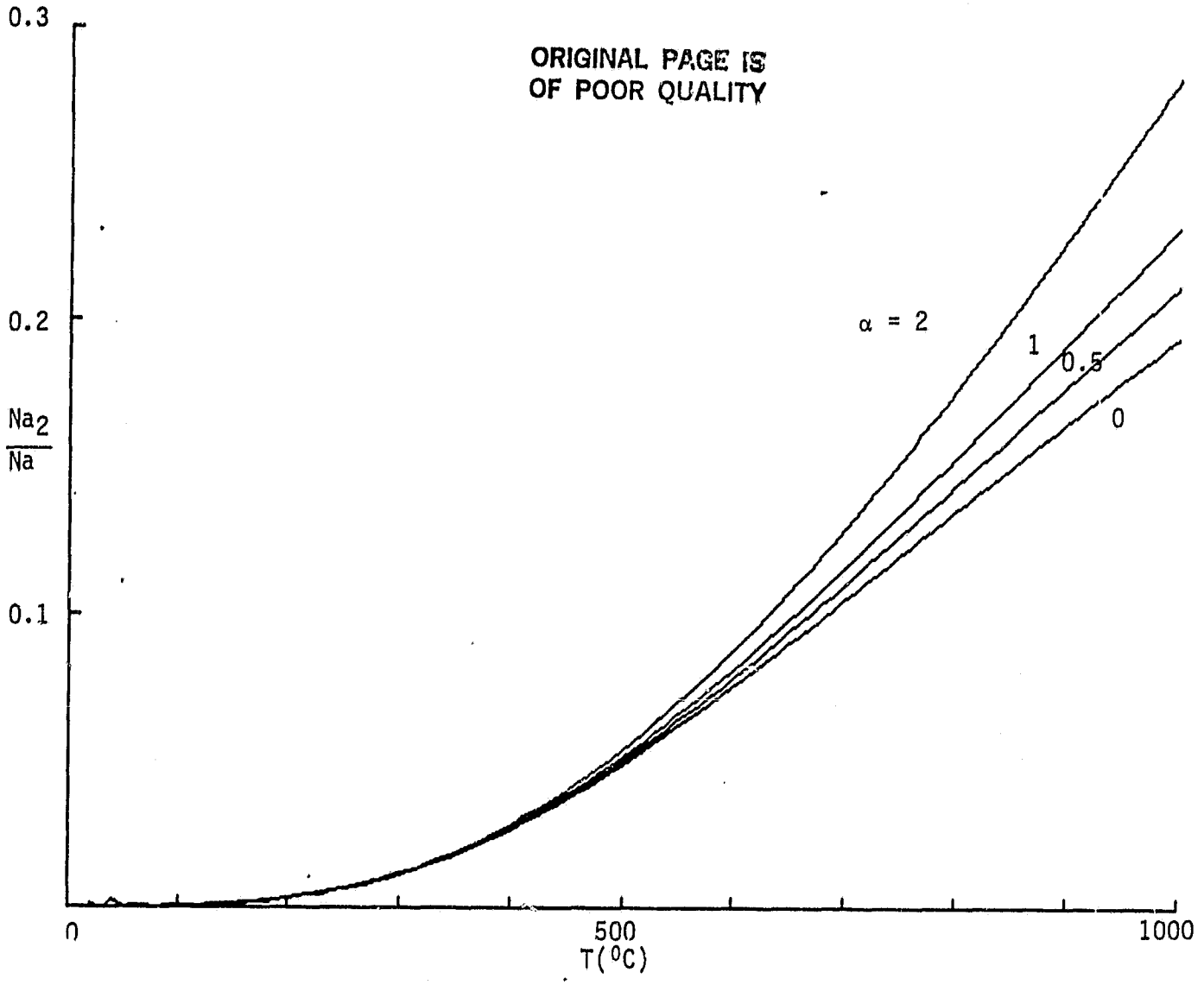

Fig. 2.2. Effect of Na_2 as a third body on the dimer/monomer ratio vs temperature. The quantity α is equal to k_s/k_r where k_s is the rate coefficient for three body recombination where Na_2 is the third body, k_r where Na is the third body. The case $\alpha = 0$ corresponds to the curve for sodium in figure 2.1. The curves were valid only up to 883°C.

III. THE POWER TO WEIGHT RATIO FOR SOLAR PUMPED LASERS

Summary

A general expression is obtained for the output power to weight ratio P_o/W, of solar pumped lasers assuming the weights of the collector and heat radiator are proportional to their areas. The ratio depends on the laser efficiency, and the temperature of the radiator. For IBr, and C_3F_7I lasers working at 600 and 650 K respectively P_o/W is five times higher for IBr than for C_3F_7I.

3.1 Introduction

One concept for the production of energy is to place solar collectors on orbiting space stations, and then transmit the energy via laser beams. Direct conversion by solar pumped gas lasers has been considered (1-3). A figure of merit, of importance for space missions, is the power to weight ratio of such laser systems.

The solar radiance is collected in a parabolic reflector and for a given output power, its area is determined by the laser efficiency. The power not converted into the laser beam must be dissipated by a heat radiator emitting by Stefan's Law; it's area depends on its temperature. Here it is assumed a functional dependence exists between weight and area of both collector and radiator.

The overall efficiency of the laser can be decomposed into the product of several efficiencies which affect the collector and radiator in different

ways. The efficiencies are described in section 3 and the energy flow is discussed in section 4. The dependencies of weight on area are then assumed which determines the weight for a given output power. Some comparisons will then be made of different laser systems.

3.2 Efficiency of Solar Pumped Lasers

As the fraction of input power which ends up as output power depends on a number of processes in the laser, it is convenient first to consider the various laser efficiences.

The overall efficiency of solar pumped lasers can be subdivided into the product of four efficiences.[1] First if absorption occurs over a bandwidth λ_1 to λ_2, the fraction of the solar spectrum used, or "solar utilization efficiency" is η_s:

$$\eta_S = \int_{\lambda_1}^{\lambda_2} \Phi(\lambda)d\lambda / \int_{o}^{\infty} \Phi(\lambda)d\lambda$$

where $\Phi(\lambda)$ is the solar radiance in watts per square meter between λ and $\lambda + d\lambda$.

The absorption efficiency η_A is that fraction of photons within the absorption bandwidth absorbed by the gas. At low pressure $\eta_A = x\sigma_a(N)d$, where x is the number of times the radiation passes through the gas by reflection, σ_a the absorption cross section, (N) the density of absorbers and d the thickness of gas. At high values of $(N)d$ the absorption efficiency approaches 1.

Of the photons absorbed, only a fraction η_K end up in producing a lasing transition and η_K is the "kinetic efficiency." Finally the quantum

efficiency η_Q is the ratio of the energy of the emitted photon to the average energy of the absorbed photons. The overall efficiency η is $\eta_S\eta_A\eta_K\eta_Q$.

3.3 Energy Flow in Solar Pumped Lasers

An idealized model for this discussion is shown in figure 1 and the energy flow is shown in figure 2, which is helpful for the following discussion. The solar radiance falls on the collector of area A_c and the power arriving at the collector is P_i. The parabolic mirror of reflectivity r concentrates the flux and a fraction rP_i reaches the first transparent wall containing the lasing medium. However a fraction $(1-r)P_i$ has been absorbed by the mirror and has to be radiated. The first container wall is assumed to have a transmittance τ_1, so the power arriving at the lasing medium is $\tau_1 rP_i$ and the power absorbed by the wall is $(1-\tau_1)rP_i$ which also has to be radiated.

Of the power arriving at the laser medium, which is distributed in wavelength over the solar spectrum, only a fraction η_S can be utilized, and only η_A of that is absorbed. The power absorbed P_A is $\eta_S\eta_A\tau_1 rP_i$ and the remainder $(1-\eta_S\eta_A)\tau rP_i$ passes through the lasing medium to the second container wall. The output power P_o is $\eta_K\eta_Q P_A$ and the part lost due to the lasing process, $(1-\eta_K\eta_Q)P_A$ has to be radiated.

The power not absorbed by the lasing medium is $(1-\eta_S\eta_A)\tau_1 rP_i$ and reaches the second wall. If the second wall has a transmittance τ_2 then $\tau_2\ (1-\eta_S\eta_A)\tau_1 rP_i$ is transmitted through it, and does not have to be radiated. An amount $(1-\tau_2)\ (1-\eta_S\eta_A)\tau_1 rP_i$ absorbed in the wall has to be

radiated.

The total power that has to be radiated is P_r:

$$P_r = Pi \{(1-r) + r(1-\tau_1) + r\tau_1 \eta_S \eta_A (1-\eta_K \eta_Q) + r\tau_1 (1-\eta_S \eta_A)(1-\tau_2)\} \quad (1)$$

The output power P_o and input power P_i are related by

$$P_o = r\tau_1 \eta P_i \quad (2)$$

and the relation between the radiated and output power is:

$$P_r = \frac{K P_o}{\eta} \quad (3)$$

where $$K = \frac{1}{r\tau_1} [(1-r) + r(1-\tau_1) + r\tau_1 \eta_S \eta_A (1-\eta_K \eta_Q) + r\tau_1 (1-\tau_2)(1-\eta_S \eta_A)] \quad (4)$$

Equation (4) contains information on the collecting mirror, the laser medium, and the transparent walls containing the medium.

3.4 Output Power to Weight Ratio

The solar radiance is $1.4\ kWm^{-2}$, and if the output power is $P_o(kW)$ then the area of the collector A_c is:

$$A_c = P_o/1.4\eta\ r\tau_1 (m^2). \quad (5)$$

The radiator emits by Stefan's Law and its area is:

$$A_r = P_r/\sigma\varepsilon T^4 \qquad (6)$$

where σ is Stefan's constant, ε the emissivity and T the temperature of the emitting surface. It is assumed that efficient conduction by heat pipes causes T to approach the working temperature of the laser.

It is also assumed that A_r is adjusted to be just sufficient to radiate the power required; at high temperatures A_r can be made correspondingly smaller.

Assumptions must now be made of the dependence of the weights of the collector and radiator on their respective areas. The collector is assumed to be either a spherical or cylindrical reflecting mirror, and its weight W_c is assumed proportional to its area:

$$W_c = \alpha A_c \qquad (7)$$

Similarly, the radiator weight W_r is given by:

$$W_r = \beta A_r^n \qquad (8)$$

The α and β are constants of proportionality and n is a constant which is included to account for the weight of the heat pipes but probably does not differ greatly from 1. It is assumed here $n = 1$.

From equations 1 through 8, the total weight W of the laser, collector and radiator is:

$$W = W_L + \frac{\alpha P_o}{1.4\eta r \tau_1} + \frac{\beta K P_o}{\eta \sigma \varepsilon T^4} \qquad (9)$$

where W_L is the weight of the laser. It is not unreasonable to assume W_L to be negligible with respect to the collector and radiator, and if so then equation 9 yields the output power to weight ratio P_o/W:

$$\frac{P_o}{W} = \frac{\eta}{\frac{\alpha}{1.4 r \tau_1} + \frac{\beta K}{\sigma \varepsilon T^4}} \quad ; \quad W_L << W \qquad (10)$$

The ratio is increased if α, $\beta \to 0$ and T is as high as possible. The dependence on the efficiencies is $P_o/W = f(x,y)$ where $x = \eta_S \eta_A$ and $y = \eta_K \eta_Q$. A plot of P_o/W on an xy plane is shown in figure 1, for τ=0.98, $\alpha = 1$, $\tau_1 = \tau_2 = 0.9$. The value 0.9 is high but achievable if the walls are either KCs or CsI.[4] The values of β are taken as 1 and 10, the latter being an extreme case for illustrative purposes. The range of x and y is only 0-0.3 corresponding to actual efficiencies in practice. The emissively ε was taken as 0.9, and the temperatures chosen are from 300 to 1500 K in steps of 300.

For both cases P_o/W either constant or increases monotonically with both x and y, and the highest P_o/W occurs in the right hand corner of the diagrams. The effect of β/α is large at low temperatures, (comparing figure 1a and 1b) and here $P_o/W \tilde{\propto} 1/\beta$. At high temperatures the T^4 depen-

dence quickly makes the area required for the radiator small and P_o/W is independent of both T and β, provided T is high.

Assuming that α and β which are determined by structure design are constants for all lasers, then equation 10 enables a comparison to be made for different lasing materials provided the various efficiencies are known. A comparison of IBr and C_3F_7I lasers is shown in table 1. It is assumed that the gas pressure and depth are sufficiently high that $\eta_A = 1$. The kinetic efficiency of C_3F_7I is assumed as 1. That of Na_2 is also doubtful. The value of $\alpha P_o/W$ is calculated from equation 10 assuming $r = 0.98$, $\tau_1 = \tau_2 = 0.9$. For $\alpha = 1$ the values of β are taken as 1 and 10. The temperatures are approximate working temperatures. Table 1 shows that the IBr laser has a power weight ratio about five times higher than the C_3F_7I laser for $\beta = 1$ and 10.

3.5 Conclusions

Assuming that a solar pumped laser has a radiation collector and heat emitter whose weights are proportional to their areas, and that the weight of the actual laser is negligible in comparison, a relationship is obtained for the output power per unit weight. This ratio, a figure of merit for solar pumped lasers acting as energy converters, seems to be about five times higher for an IBr than a C_3F_7I laser.

Table I

Comparison of Various Lasing Materials in Solar Pumped Lasers

Material	η_S	η_A	η_K	η_Q	η	T(K)	P_o/W	
							$\beta=1$	$\beta=10$
IBr	0.12	1	0.57	0.18	1.2×10^{-2}	600	9.4×10^{-3}	4.1×10^{-3}
C F I	10^{-2}	1	1	0.22	2.2×10^{-3}	650	1.75×10^{-3}	1.44×10^{-3}

REFERENCES - SECTION III

1. Harries, W.L. and J.W. Wilson. Space Solar Power Review, 2:367 (1981).

2. Harries, W.L. and W.E. Meador. Kinetic Modeling of an IBr Solar Pumped Laser. Space Solar Power Review, in press.

3. Lee, J.H. and W.R. Weaver. Appl. Phys. Lett. 39:137 (1981).

4. Taussing, R., Bruzzone, C., Nelson, L., Quimby, D. and Christiansen, W. Proceedings of the AIAA Terrestrial Energy Systems Conference, Orlando, Florida, June 4-6, 1979.

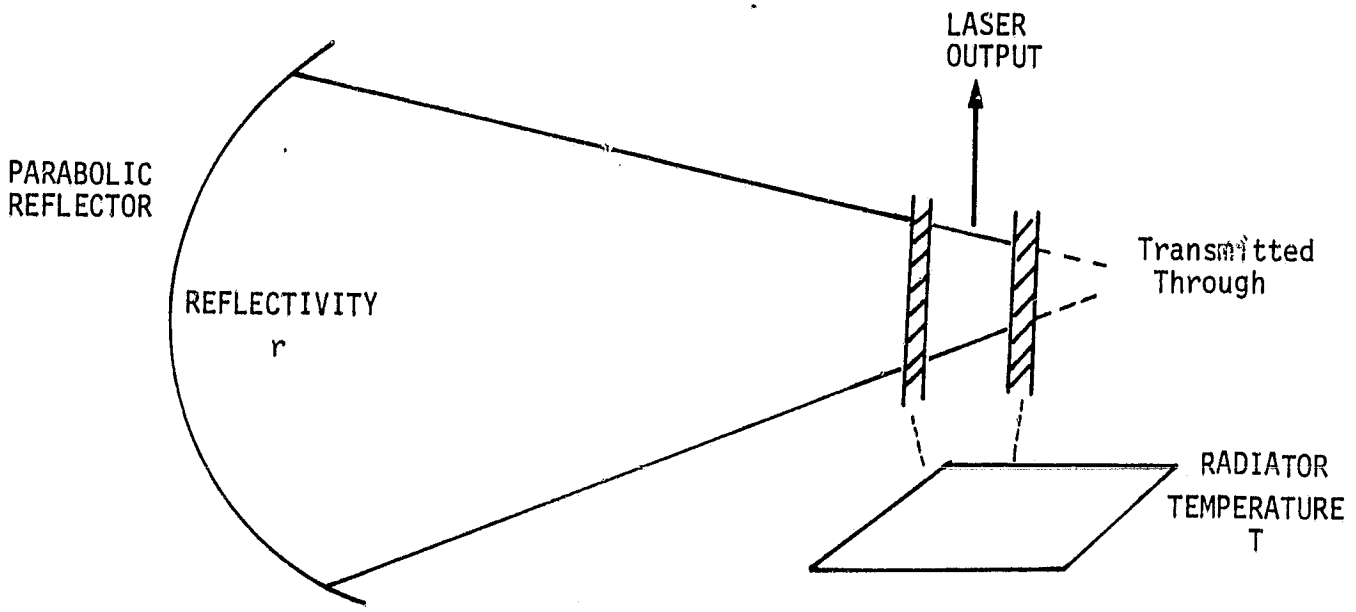

Fig. 3.1. Idealized arrangement for a solar pumped laser.

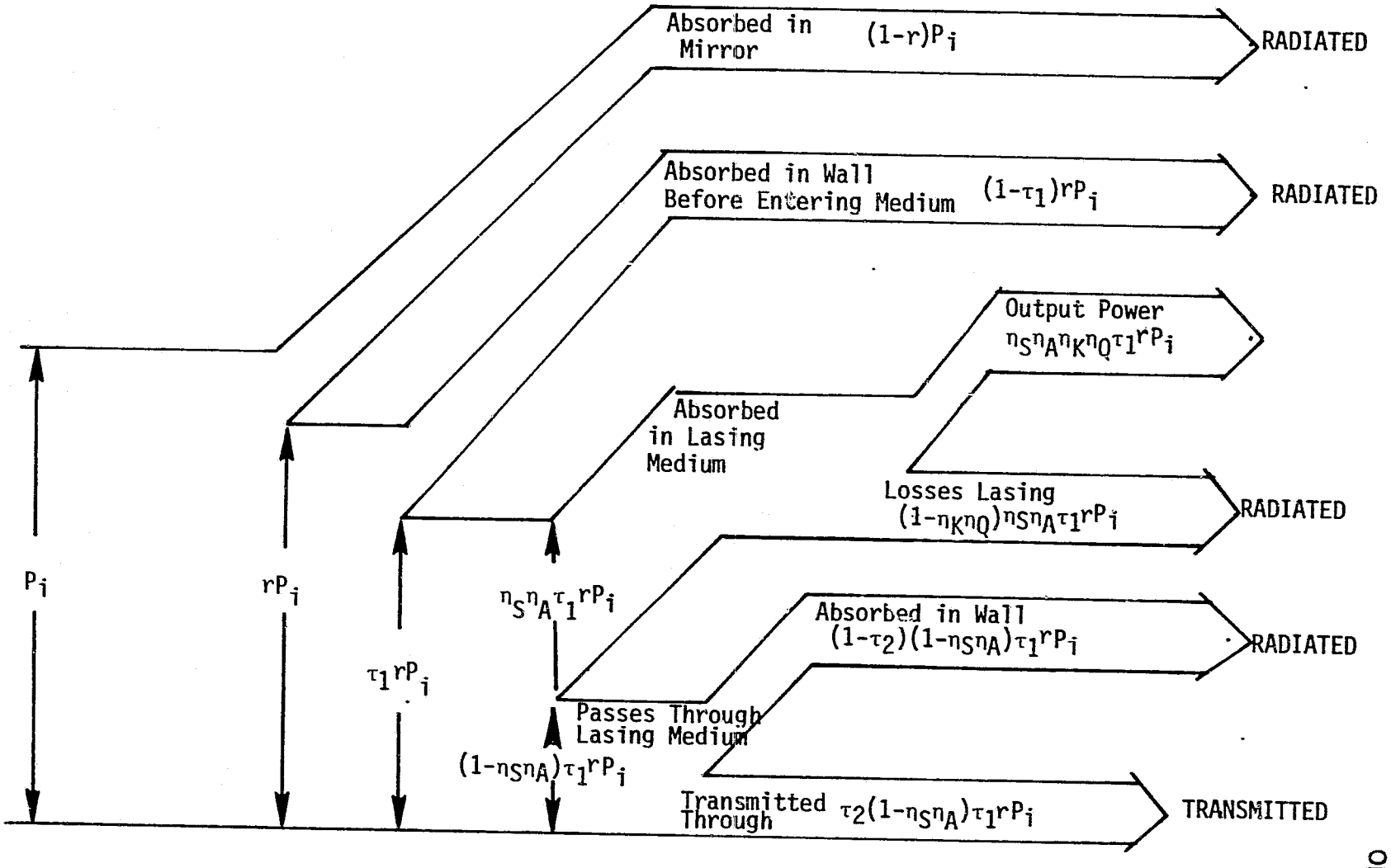

Fig. 3.2. Energy flow chart for a solar pumped laser.

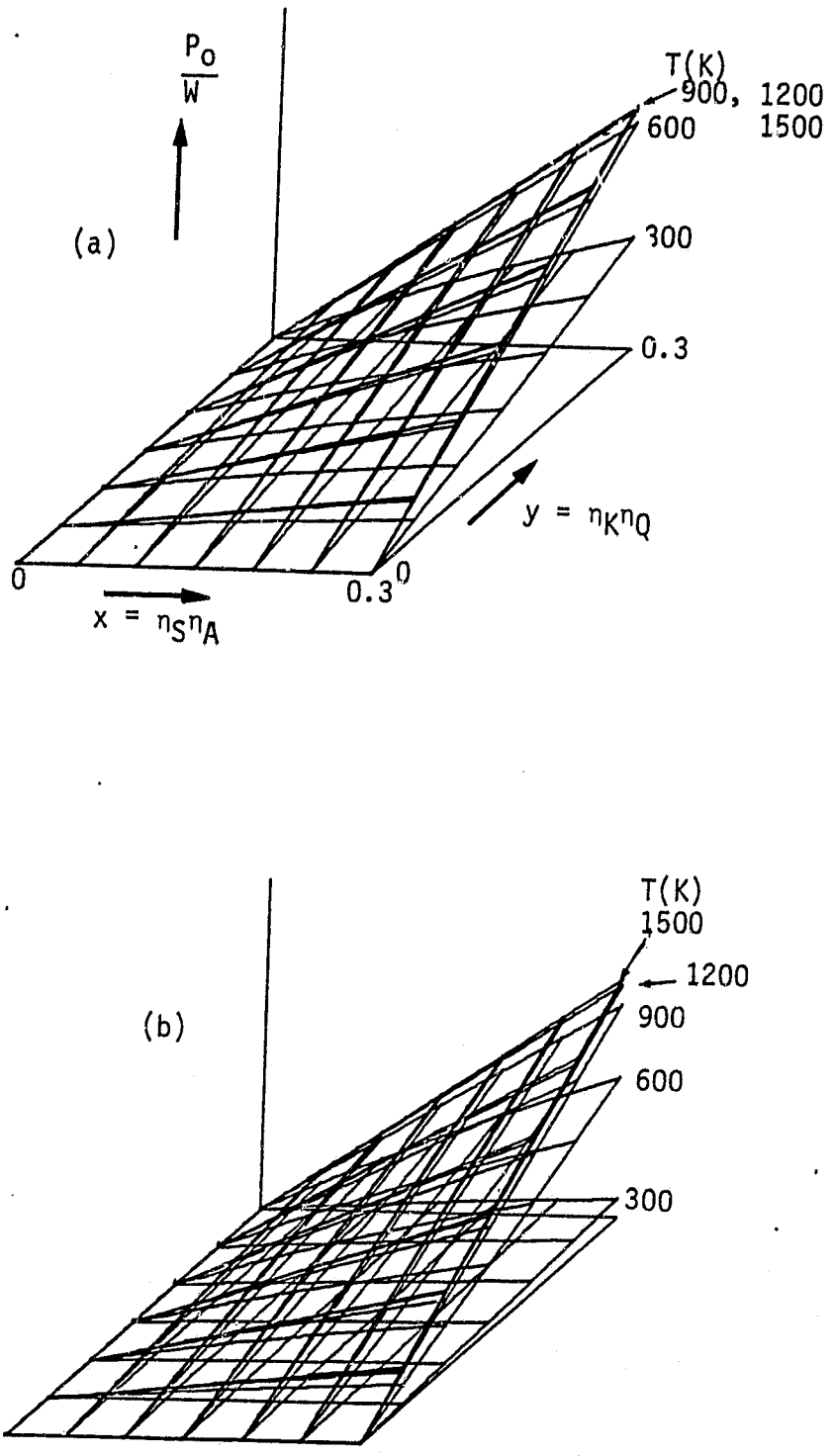

Fig. 3.3. Plot of P_o/W on an x, y plane for different temperatures showing effect of varying β/α. Values assumed are $r = 0.98$, $\alpha = 1$, $\tau_1 = \tau_2 = 0.9$. (a) $\beta = 1$, (b) $\beta = 10$ an extreme case.

IV. A LIMITATION IN SCALING UP A BLACK BODY LASER

Summary

A black-body pumped CO_2+ buffer gas laser is assumed cylindrical of length L and radius r. The pumping rate is determined by the rate of arrival of radiation in a bandwidth 0.1μ at the laser surface according to Planck's radiation formula. The power input per unit volume however is proportional to 1/r. A maximum value of r is determined from experimental results for threshold at 1500 K. Increased power can only be achieved by increasing L which becomes impossibly large. The limitation can be circumvented by a box type laser.

4.1 Introduction

The purpose of this paper is to illustrate a limitation on the pump power input into a black body laser if the geometry is cylindrical.[1] The input energy flux is limited by Planck's radiation formula, and there is no means of concentrating it, as would be done by parabolic solar reflectors. The pump power per unit volume is estimated from the experimental results of Insuik et al.[2] To attain a given power input per unit volume it will be shown that there is an upper limit to the radius. Hence in scaling up to large power output, a cylindrical laser turns out to be impossibly long. A method of overcoming the limitation using a box laser geometery is given.

4.2 Absorption of Black Body Radiation

Experiments have shown that for a CO_2 black body laser, with a buffer gas, absorption occurs at 4.256 μ with a bandwidth of 0.1 μ.[1] The lasing medium in the form of a cylinder of radius r and length L receives energy from the black body cavity at a rate per unit surface area given by Planck's radiation formula

$$E(\lambda)\, d\lambda = \frac{3.74 \times 10^{-12}\, d\lambda}{\lambda^5 (\exp \frac{1.439}{\lambda T} - 1)} \text{ watts cm}^{-2} \qquad (1)$$

where λ is the wavelength, $d\lambda$ the absorption bandwidth both in cm and T the temperature in degrees Kelvin. For the above wavelength and bandwidth:

$$E(\lambda)\, a\lambda = \frac{2.68}{\exp (\frac{3381}{T}) - 1} \text{ watts cm}^{-2} \qquad (2)$$

a function of temperature only.

The power entering the laser medium is then $E(\lambda) \cdot 2\pi rL$ but to obtain the power P entering unit volume on the average we must divide by $\pi r^2 L$, or

$$P = 2E(\lambda) d\lambda / r \qquad (3)$$

Hence increasing r, decreases P, and there is a limitation on r, which has a maximum value given by equation (3) when P is just sufficient for threshold. To scale up for high power output, (for a given efficiency)

the only remaining alternative is to increase L.

Some illustrative values of $E(\lambda)d\lambda$, and P, are shown in table I, where r is assumed to be 1 cm.

Table I. Values of $E(\lambda)d\lambda$, the power per square cm and P, the power per cc vs temperature.

Black Body temp K	$E(\lambda)d\lambda$ watts cm^{-2}	P watts cm^{-3}
1000	0.094	0.188
1100	0.130	0.260
1200	0.170	0.340
1500	0.314	0.628
2000	0.606	1.212
3000	1.285	2.569

4.3 Estimate of Threshold Input Power

An approximate estimate of the pump power per cc to attain threshold can be obtained from the experimental results of Insuik et al.[2] Their experiment was done in a sapphire tube of internal diameter 8 mm outside diameter of 9.5 mm, with 50 cm of its length in a hot zone. The medium was CO_2 with He and Ar as buffer gases. Lasing occurred with the black body temperatures ranging from about 1100 to 1500 K.

By varying the pressure it was found that a drop off in power occurred around 7 torr total pressure when there was 21% CO_2, suggesting that the pressure and path length were just great enough to absorb all the input radiation. Assuming the absorption length L' to be of order 0.8 cm, this leads to an absorption cross section $\approx 3\times10^{-17}$ cm^2 and a relation between the path length and CO_2 pressure:

$$L' p \approx 1 \text{ (cm torr)} \qquad (4)$$

where $L = 2r$ is in cm, and p in torr for maximum output. Neither the pressure of CO_2 nor r can be increased indefinitely in scaling to higher power, otherwise the radiation will not penetrate to the center of the tube. If Lp is too small the radiation will not be absorbed.

A very rough estimate of the pump power per cm^3 for threshold can be made. A number of experiments[2] showed that maximum output power occurred over a narrow range of total pressures P_t ; $25 < P_t$ 12.5, and CO_2 pressure p; $0.5 < p < 2.5$ cm. A laser power output vs. temperature curve for $P_t = 7$ torr, $p = 1$ torr showed that threshold occured around 1100° and the power output rose linearly to a value of 4 mW at 1500 K. Assuming 1100K to be the threshold temperature for $r = 0.4$ cm, then equation (3) gives the minimum power per cm^3 for threshold to be $P_{min} = 0.65$ watts cm^{-3}.

Now P_{min} may not be a constant value if r is varied; increasing r decreases wall losses. Assuming it is correct in order of magnitude then the maximum value of r is obtained from equation (3)

$$r_{max} = 2E(\lambda)d\lambda/P_{min} \qquad (5)$$

with $P_{min} = 0.65$ watts cm^{-3}, e.q. at $T = 1100°$ $r_{max} = 0.4$ cm, and at 1500°C $r_{max} = 1$ cm.

4.4 Power Output and Laser Dimensions

If the overall efficiency of the laser is n then the power output P_o is

$$P_o = \eta \, 2\pi rL \int E(\lambda) d\lambda \qquad (6)$$

and increases with rL for a given cavity temperature T. To increase P_o r should approach r_{max}, determined for given T from equation (6). Then given η, L can be calculated; e.g. for P_o = 10KW, T = 1500 K, η = 0.1 r_{max} = 1 cm, then L = 500 m for a laser tube of 1 cm radius. The length L is impossibly large.

The difficulty can be overcome by a box laser arrangement (Fig. 1) when the medium is in the form of a flat plate. The output power is now

$$P_o = 2 \eta \, xy \int E(\lambda) d\lambda \qquad (7)$$

the factor 2 arising as it is pumped from two sides. Using the same numbers as above then $xy = 16\ m^2$, or $x = y = 4m$, much more reasonable values.

4.5 Conclusions

In scaling up a black body cavity laser to high powers, there is an inherent limitation because the energy flow into the laser medium is limited by the Planck radiation formula. Concentrating it by parabolic reflectors does not seem possible. In addition the power input per unit volume varies inversely as the radius if the medium is cylindrical and the value of the radius is limited by a threshold condition. For high power the length L must therefore be increased to a value impossibly large.

The limitation can be overcome by using a box laser arrangement, which essentially offers a greater area for pumping in a much more compact arrangement.

REFERENCES - SECTION IV

1. Taussig, R., Bruzzone, C., Nelson, L., Quimby, D., and Christiansen, W. AIAA Terrestrial Energy Conference, June 4-6, 1979, Orlando, Florida.

2. Insuik, R.J., Christiansen, W.H., Private communication, submitted to Journal Quantum Electronics.

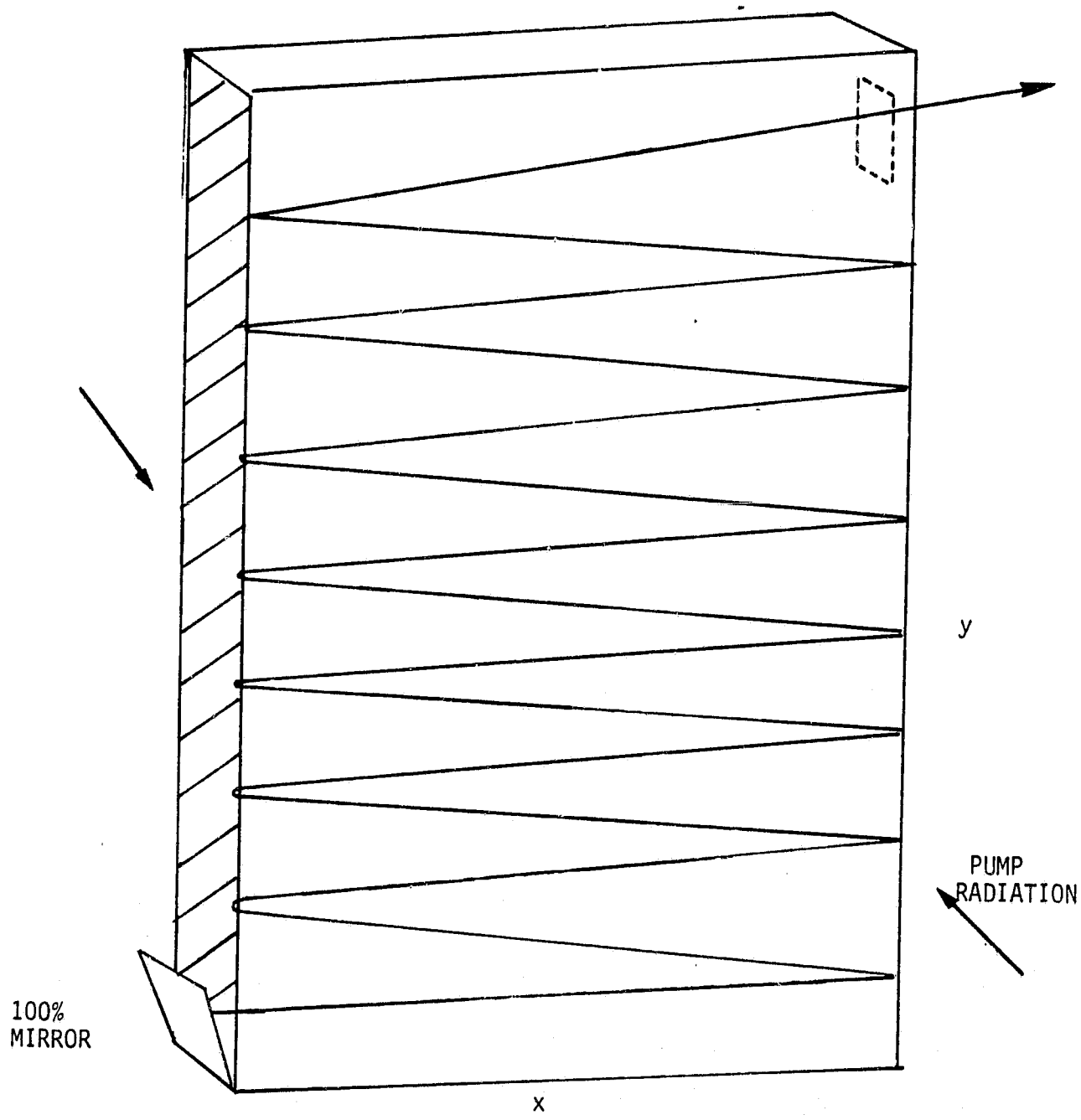

Fig. 4.1. Box laser arrangement.

V. OVERALL CONCLUSIONS

The study of stimulated emission/absorption for Na_2 indicated that there was a region around 520 nm where the emission/absorption cross section ratio was very high, and lasing should be attempted here. The dimer/monomer ratio of a number of vapors was investigated as a function of the temperature. The fundamental processes were elucidated, and the results agreed well with previous ones and showed that the ratio increased monotonically with temperature. Improved calculations on the power to weight ratio indicate that this figure of merit would be about five times greater for an IBr than for a C_3F_7I laser. Lastly, a limitation in the scaling of black body lasers to higher power was studied, and it was shown that higher powers could only be achieved in a box laser configuration, rather than a cylindrical geometry.

ACKNOWLEDGMENTS

The authors gratefully acknowledge many useful discussions with Dr. W. E. Meador, and thank Mr. W. Weaver for his considerable help.